University of Baghdad
College of Engineering
JOURNAL OF ENGINEERING

Journal of Engineering

journal homepage: www.jcoeng.edu.iq

Volume 32 Number 8 August 2026

Beyond the Optical Limit in p-18O Collisions: Glauber Model Calculations with Woods-Saxon and Sharp-Sphere Density Distributions

Israa Ali Madhi *, **Basim Khalaf Rejah**

Department of Physics, College of Science for Women, University of Baghdad, Baghdad, Iraq

ABSTRACT

This study investigates high-energy proton–oxygen collisions ($\sqrt{s_{NN}}$=0.056) using the Optical Glauber Model and accounts for how different nuclear density distributions affect the properties of the collision both geometrically and dynamically. The Glauber Model is a very common technique in heavy-ion physics that treats nuclei as continuous matter distributions; however, the effect on proton–nucleus systems of adopting different nuclear density distributions remains insufficiently studied, especially the Woods–Saxon and Sharp-Sphere distributions. In this regard, oxygen nuclei were selected because their low mass makes them an important reference system that has rarely been considered for comparison in the past. This work provides a systematic comparison of these two density distributions by computing several observables such as the thickness and overlap functions, the number of participating nucleons, and the number of binary collisions. It is observed from the results that the Woods–Saxon distribution produces a relatively smoother and wider overlap geometry along with a larger N_{part}, while the Sharp-Sphere distribution provides steeper behaviour to all observables as the collision impact parameter increases. In both cases, the N_{part} and the N_{coll} decrease with a higher collision impact parameter, owing to a shrinking nuclear overlap region. These results demonstrate a significant sensitivity of the collision geometry on the presumed method of specifying the nuclear density distribution, as well as emphasize that precise models of nuclear structure are essential to describing properties of the initial state in high-energy p-18O interactions.

Keywords: Heavy ion collisions, High energy, Nuclear density, Nuclear radius, Quark-Gluon plasma.

1. INTRODUCTION

A comprehensive study of quark-gluon plasma (QGP) cannot be performed in a research laboratory because of the thermodynamic circumstances required, except for large-scale experimentation that can stimulate particle beams up to relativistic speeds before they strike **(Kasza, 2026)**. An exemption is a hadronic collision, which is a complex process in

*Corresponding author
Peer review under the responsibility of University of Baghdad.
https://doi.org/10.31026/j.eng.2026.08.12
This is an open access article under the CC BY 4 license (http://creativecommons.org/licenses/by/4.0/).
Article received: 28/02/2026
Article revised: 29/06/2026
Article accepted: 08/07/2026
Article published: 01/08/2026

which QGP constitutes only a brief component of the relevant physics. Currently, the production of (QGP) can only be achieved through Heavy Ion Collisions (HICs)**(Mattioli, 2024; Nguyen, 2020)**. Each stage of the collision has different characteristics, but all are governed by the Lorentz-invariant proper time, where τ =0 is the time of collision **(Iancu, 2012; Andronic and Arnaldi, 2025)**. In collisions involving heavy nuclei, such as Pb–Pb **(Perepelitsa, 2024)** and Xe–Xe, significant energy dissipation has been documented, with indications of non-negligible energy loss even in smaller systems like p–Pb. These findings prompt an inquiry into the system size necessary for the generation of a quark–gluon plasma **(Kumar and Shukla, 2024)**. Within this context, O–O And p–O collisions are of particular interest. Oxygen characterized by equal atomic numbers and neutron numbers Z = N = 8, represents a balance and relatively light nuclear system. Making it suitable for investigating size-dependent effects. p–O collisions have yet to be detected in a quark-gluon plasma state **(CMS Collaboration, 2025)**. Moreover, Proton-oxygen (Proton-O) collisions are essential for comprehending and analyzing nucleus-nucleus data. Consequently, proton-nucleus collision at elevated energies provides an opportunity to examine how the mechanisms of light and hard scattering interaction, along with subsequent particle creation, are influenced by a greater nuclear target **(Salgado et al., 2011)**. To examine the impact of nuclear effects in proton-O collisions, it is crucial to characterize p-A collisions, where there is a decrease in the proton components, resulting in a diminished rate of nucleon-nucleon interaction due to a reduced number of conflicting events between the projectile and the target nucleus **(Alvioli et al., 2014; 2017)**. Such collisions influence the quantity of nucleons impacted within the target nucleus. The initial O–O and p–O collision experiments were performed at the LHC in 2025, with a center-of-mass energy of $\sqrt{s_{NN}}$=5.36 TeV per nucleon pair **(CMS Collaboration, 2025)**. Experimental findings at the LHC have demonstrated that theoretical analyses are both predicted and essential, hence justifying the application of the optical Glauber model as a standard instrument. This model enables the characterization of the colliding particles' structure and the starting geometry of high-energy collisions **(Eskola et al., 2017)**. Accordingly, this work aims to generate predictions for the proton-O collision at the nucleon-nucleon center of mass system energies $\sqrt{s_{NN}}$=0.056 TeV. The hadron production rate is associated with nucleon-nucleon reaction time, as experimentally demonstrated **(Liu et al., 2022)** through variations in energy and momentum. For this reason, our calculation will predominantly depend on the Woods-Saxon and Sharp Sphere density distributions, considering the σNN influence on the density of the two nuclear particles.

The Glauber model offers a quantum framework for elucidating scattering at elevated energy. It utilizes the Eikonal approximation, which considers the colliding nucleons of both the projectile and target as following linear paths **(Aaij et al., 2022)**. This model allows for the calculation of total, elastic, and inelastic cross sections. The objective of modelling is to ascertain the positions of nucleons through nuclear density distributions, including Woods–Saxon and hard-sphere models **(Mehndiratta and Shukla, 2017)**. and for the optical limit of the Glauber model, nuclei are regarded as continuous density distributions, facilitating the computation of quantities such as N_{part} (number of participating nucleons), N_{coll} (number of binary collisions), and the pertinent cross sections, while disregarding event-by-event fluctuations and nucleon correlations **(Miller et al., 2007)**.

This work aims to investigate the influence of the nuclear density distribution on the geometrical properties of proton–oxygen18 collisions at $\sqrt{s_{NN}}$ =0.056 TeV within the framework of the Optical Glauber Model. A comparative study based on the Woods–Saxon and Sharp Sphere density distributions is carried out to evaluate their effects on the calculated geometrical observables, including the impact parameter, the number of participant nucleons, the number of binary collisions, and the nuclear overlap function.

2. MATERIALS AND METHOD

2.1 Wood-Saxon Distribution

This distribution has a gradually decreasing density from the center to the edge. Glauber proposed that the collision of two nuclei remains undeflected at high energy, leading to an impact-parameter-characterized linear path. This defines the level of centrality. The overall number of interactions among participants' nucleons is denoted by the number of collisions which occur in a specific event **(Shukla, 2001b)**. In collisions involving spherical-symmetric nuclei and very high-energy heavy ions, the Fermi distribution, also known as the Woods-Saxon density distribution, quantifies the nucleon density per unit volume. It is commonly utilized to determine nucleon density and is applied as a nuclear profile, expressed as follows **(Loizides et al., 2018; Krupczak et al.,2025)**:

$$\rho_{A^{(r)}} = \rho_0 \frac{1+\omega(r/R)^2}{1+exp\left(\frac{r-R}{a}\right)} \tag{1}$$

The general normalization factor is given by $\rho_0(\text{fm}^{-3})$, which represents the nucleon density at the center of nuclei. R(fm) is the nuclear determinant radius, meaning that no nucleons exist farther than R. a is the thickness in (fm), and ω is the spherical shape deviation. This formula includes changes to take into consideration the number of nucleons: $4\pi \int_0^\infty b^2\, d\vec{b}\, \rho_0(\vec{b}) = A$, which will be utilized in our computations **(Ali and Mohammed, 2022)**. Assuming two nuclei (A and B) collide at a relativistic velocity, two flux tubes account for the displacements $\vec{s}$ and $\vec{s} - \vec{b}$, relative to the center of the target and projectile, respectively. The optical measurements depend on the thickness function, which illustrates the transverse nucleon density and refers to the integrated density across the longitudinal z-axis of the incident beam.

It signifies the number of NN collisions that the nucleon encounters when moving within the nucleus at impact parameter (b) **(Nasim et al., 2017; Ramasubramanian, 2021; Ali and Ali, 2025b)**, i.e.,

$$\int dz\, \rho_A(\vec{b}, z) \tag{2}$$

We can refer to the nuclear overlap function as the probability per unit volume $\rho_{A,B}(\vec{s}, z_{A,B})$ of two ions, which is normalized to unity to determine the nucleon at the position $(\vec{s}, z_{A,B})$. The integration across the two transverse dimensions results in **(Kuttan et al., 2023)**:

$$T_{AB}(\vec{b}) = \int T_A(\vec{s}) T_B(\vec{s} - \vec{b})\, d^2 s \tag{3}$$

The normalization is performed by the integral $\int d^2b\, T_{AB}(\vec{b}) = AB$ overall (b), $(\vec{s})$, and $(\vec{b})$ are perpendicular to the beam z-axis direction. This thickness function is a pure geometric factor that refers to the occurrence of interactions, $T_{AB}\sigma_{NN}^{inel}$ **(Jia, 2009)**

Nucleons that have engaged in at least one collision with other nucleons are classified as participants. The mean number of participants in d-A collisions at an impact parameter (b) can be calculated using this formula **(d'Enterria and Loizides, 2021; Kuttan et al., 2023)**:

$$N_{PartAB}(b) = \int d^2s\, T_A(\vec{s}) \left\{1 - \left[1 - \frac{\sigma_{NN} T_B(\vec{s}-\vec{b})}{B}\right]^B\right\} + \int d^2s\, T_B(\vec{s}) \left\{1 - \left[1 - \frac{\sigma_{NN} T_A(\vec{s}-\vec{b})}{A}\right]^A\right\} \quad (4)$$

The overall number of participants is thereafter obtained as follows **(d'Enterria and Loizides, 2021)**:

$$N_{PartAB}(b) = \int d^2s\, T_A(\vec{s}) \left\{1 - e^{-\sigma_{NN} T_A(\vec{s}-\vec{b})}\right\} + \int d^2s\, T_B(\vec{s}) \left\{1 - e^{-\sigma_{NN} T_B(\vec{s}-\vec{b})}\right\} \quad (5)$$

Local density fluctuation in the Optical Glauber Model is disregarded; every projectile nucleon behaves as a flux tube during its interaction with the incoming target. The nucleus seems like a continuous matter distribution lacking borders or density variation (smooth density). The entire cross-section for d-Au collisions, in which at least one NN collision occurs, is referred to as the total geometric cross-section and is expressed as **(d'Enterria and Loizides, 2021)**:

$$\sigma_{geo} = \int d^2b\left[1 - e^{-T_{AB}(b)\sigma_{NN}}\right] \quad (6)$$

2.2 Sharp-Sphere Distribution

The sharp sphere model, which describes the density distribution as a step function that maintains a constant density inside the nuclear radius and decreases to zero outside of it, may be used to describe the collision's density profile. The nucleon density as a function of the radial distance (r) from the nucleus center is represented by the symbol ρ_A (r) **(Mifsud, 2013)**:

$$\rho(r) = \begin{Bmatrix} \rho_0 & , r < R \\ 0 & , r \geq R \end{Bmatrix} \quad (7)$$

Where (ρ_0) represents the constant nucleon density within a unit volume of the nucleus, $\rho_0 = \frac{3A}{4\pi R^3}$, represents the nuclear radius, with the assumption $R = R_0 A^{1/3}$, (R_0 ~1.12 fm).

The sum of the densities of individual particles and their normalization forms is the total density distribution of the nucleus, denoted as ρ(r) **(Brueckner et al., 1968)**

$$\int \rho(r) d^3r = A \quad (8)$$

The thickness function, integrated along the longitudinal z-axis direction, describes the density of nucleons moving through the nuclear density. As a result, the thickness function's integral is written as: $\int d^2b T_A(b) = A$. The thickness function for sharp-sphere density is defined as the product of the densities and the path length as **(Mifsud, 2013)**:

$$T_A(b) = 2\rho_0\sqrt{R^2 - b^2};\ \text{when } b \to 0 \text{ that lead to } T_A(b) = 2\rho_0 R \quad (9)$$

The integral overlap function is the product of the two nuclear collision thickness functions defined by the overlap function **(Wong, 1994)**:

$$\int d^2b\, T_{AB}(b) = AB \tag{10}$$

While short-range correlations influence nuclear interaction and overlap functions, the overlap function is the principal value for characterizing collision strength, as it involves the thickness function. For a sharp sphere distribution, the overlap function is defined as **(Segal, 2023)**:

$$\int T_{AB}(b) = 2\pi R^4 \rho_0^2 \tag{11}$$

The overall geometric cross section for two colliding nuclei, which is stated as follows, shows that at least one nucleon-nucleon collision occurred.

$$\sigma_{geo} = \int d^2b[1 - e^{T_{AB}(b)\sigma_{NN}}] \tag{12}$$

The total number of nucleons in a nucleus, which is equivalent to the number of participants, can be directly estimated using the sharp sphere model **(Segal, 2023)**

2.3 Differences between Optical and Monte Carlo Glauber Methods

The optical limit of the Glauber Model depends on a continuous density approximation, wherein nucleons interact with the target as though it were a homogeneous and uniform medium. This mean-field-like description streamlines the formalism and gives analytically manageable formulas. In these circumstances, its predictions tend to coincide with those obtained from a more detailed probabilistic analysis **(Miller et al., 2007)**.

On the other hand, the Glauber Monte Carlo (GMC) method provides a small, spatially detailed description of the individual collision geometry. It explicitly incorporates different locations of nucleons and local density variations. As a result, contributions that are absent in the optical-limit framework, such as shadowing effects arising from the actual spatial arrangement of nucleons in the nucleus, are implemented into GMC calculations. These supplementary effects typically result in a decrease in the total cross section relative to optical-limit estimates, particularly when the nucleon–nucleon cross section is not exceedingly small **(Miller et al., 2007)**. Although these conceptual distinctions, fundamental geometric observables, such as the number of participants (N_{part}) and the number of binary collisions (N_{coll}), as functions of impact parameter, exhibit relatively small variations between the two methodologies throughout most of the impact parameter spectrum. Notable discrepancies occur primarily at very large impact parameters, where peripheral impacts exhibit heightened sensitivity to microscopic structure and oscillations.

The optical limit efficiently and robustly describes average geometric trends, while the Glauber Monte Carlo method gives enhanced accuracy for total cross-section computations, event-by-event fluctuations, and analyses sensitive to nuclear substructure. The selection between the two methods is dependent upon the particular observable being examined and the requisite degree of precision **(Loizides et al., 2015)**.

3. RESULTS AND DISCUSSION

To evaluate the overlapping variables, we perform tests at two different potentials, Woods-Saxon and Sharp Sphere, at one high energy $\sqrt{s}$ =0.056 TeV and using the inelastic nucleon-nucleon cross section σ_{NN} =37 mb derived from a logarithmic interpolation of cross-section measurements related to collision energies **(Ali and Mohammed, 2022)**. Utilizing the

Optical Glauber approach and impact parameter b =2 fm, the estimation of the geometrical parameter (N_{coll}, T_{AB}) and others is often conducted using the "overlap" program written in Fortran 90.

The nuclear density as a function of nuclear radius b for p-O collision, based on the Woods-Saxon distribution and sharp-sphere at 0.056 *TeV* and 37 *mb*, is illustrated in **Fig. 1**.

The Woods-Saxon distribution is a mathematical framework that clarifies the variance in densities within the nucleus. This is a frequently employed approximation of the actual value, a more complex nuclear density shape. **Fig. 1-a** aligns with the expected distribution of nuclear density, reaching its peak toward the nucleus center. The heightened density arises from the strong nuclear force that binds the particles, gradually decreasing in a consistent manner, in accordance with the bell-shaped curve (Gaussian distribution) of the model, and then declining as it extends further from the center.

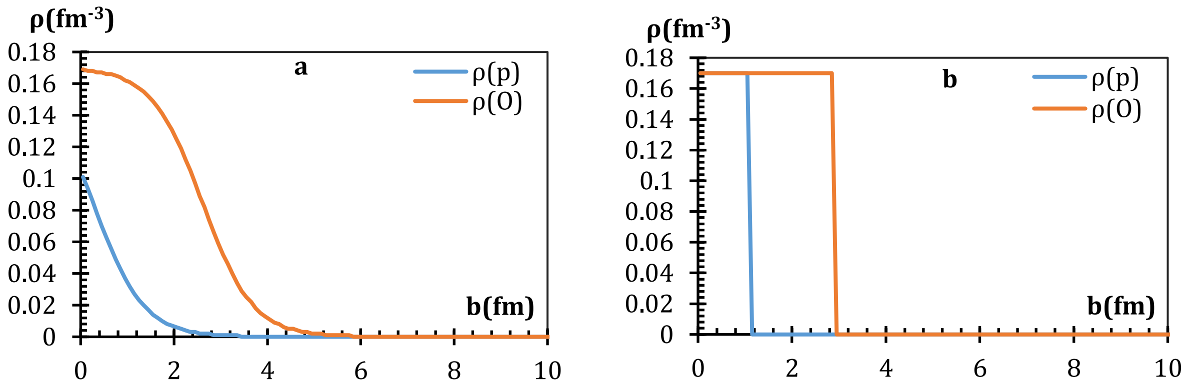

Figure 1. Nuclear density for p-O collision at 0.056 *TeV* and 37 *mb* according to the (a) Woods-Saxon distribution and (b) Sharp-Sphere distribution.

Fig. 1-b shows that the densities maintain an approximate consistency at the value ρ~0.17 fm^{-3} within their respective nuclear radii and decline abruptly to zero after these boundaries, indicating a sharp sphere density profile. The proton density reduces at a lower impact parameter than oxygen, reflecting its smaller effective radius, while the oxygen densities extend to greater b values because of the bigger diameter of the oxygen nucleus. This behavior illustrates the geometric variation between the projectile and the target nuclei, demonstrating the significance of nuclear size in defining the overlap geometry and subsequently the contact region in p-O collisions.

Fig. 2 illustrates the thickness density curve, also known as the collision function, for proton-oxygen collisions with an energy of 0.056 *TeV*.

The thickness density function is an essential tool for analyzing nuclear collisions. It can be employed to calculate the probability of certain reaction channels occurring, including the generation of new particles. The thickness function typically demonstrates behavior like the bell shape of the Gaussian curve. The function has a large value at a small impact parameter (b), showing a high probability of interaction where the nuclei are close to each other. And when the value of (b) grows, the function's value diminishes, indicating a reduction in the probability of the reaction. This also relates to the centrality of the collision, denoting the proximity or farness of the nuclei to one another.

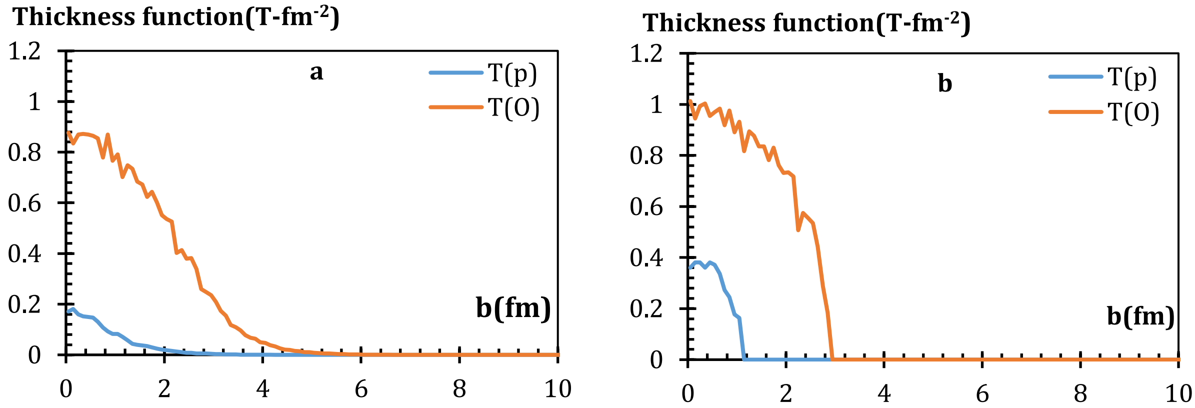

Figure. 2. The thickness density function T for p-O collision (a) Woods-Saxon distribution and (b) Sharp-Sphere distribution

Fig. 2-a shows that the Woods–Saxon density distribution produces a thickness function that diminishes gradually with increasing impact parameter, approaching zero at approximately 5 fm. This behavior reflects the diffuse nature of the nuclear surface and the gradual reduction of the overlap region between the colliding nuclei. Conversely, the thickness function obtained from the sharp-sphere density distribution, **Fig. 2-b**, declines more steeply and approaches zero at approximately 3 fm, due to the assumption of a sharply defined nuclear boundary. The differences highlight the impact of the adopted density profile on the overlap geometry and, consequently, on the collision probability in proton–oxygen interactions. This outcome is intuitively logical, as it represents the minimum proximity between two nuclei without any actual overlap. The failure of the thickness function to attain zero at exactly zero impact parameter signifies that proton and oxygen nuclei have a definite size. Given that the function is normalized to unity, the integral of the thickness function over all possible impact parameters equals one **(Ali and Ali, 2025a)**.

In general, **Fig. 3** illustrates that the optical Glauber model can, in principle, compute the overlap function and use it to find the collision probability in a p-O collision at two distinct distributions for one energy, 0.056 *TeV*, based on nucleon density and reaction energy.

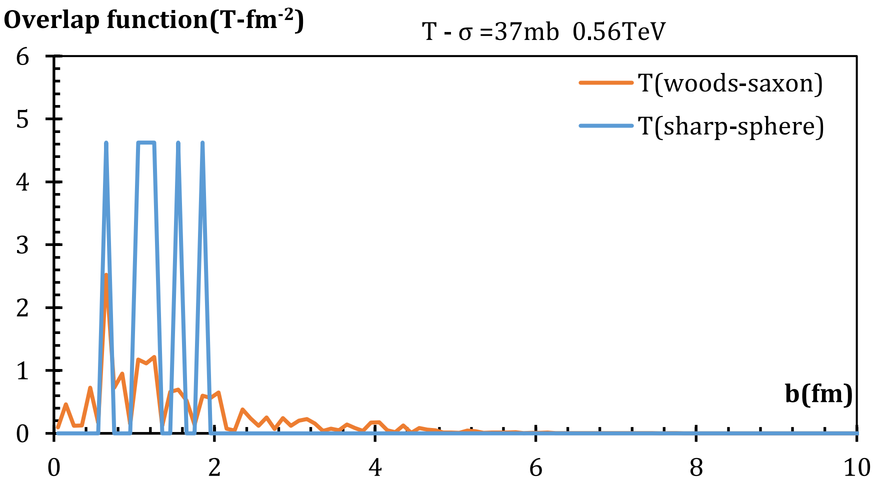

Figure 3. Nuclear overlap function in $T_{P\text{-}O}$ collisions at different distributions

The Woods-Saxon distribution indicates a more gradual pattern. When the impact parameter increases, the overlap function diminishes progressively because of the diffuse features of the nuclear surface. Minimal values of the impact parameter (b ≤ 2 *fm*) refer to central collisions, where nuclear overlap maximizes, while the greater values of (b) result in the disappearance in overlap, indicating peripheral collisions. Conversely, in the Sharp-Sphere distribution, the overlap function stays nearly constant until the impact parameter nears the nucleus radius; at that moment, it rapidly declines to zero. This significant decline illustrates the physical principle of this concept **(Ali and Ali, 2025a)**.

Fig. 4 shows N_{part}, the number of participant nucleons at the chosen distribution. The diverse lines in **Fig .4** represent distinct collision energies and inelastic cross sections. As the effect parameter (b) decreases, the number of nucleons participating in the experiment usually increases. A more direct collision is the outcome of a drop (b). As a result, more nucleons from the projectile will interact with nucleons from the target (^{18}O). The reaction area is where the projectile (p) and (^{18}O) nucleons contact during a collision, leading to the exchange of more nucleons. When the impact parameter was reduced, the oxygen nucleon sharing lines increased more sharply than the emitted sharing lines. The interpretation is that the reaction area within the oxygen nucleus permits a greater number of nucleons to participate in straight collisions (the impact parameter is small). Impact energy, in general, has a smaller effect on the number of participating oxygen nucleons than it does on the number of nucleons that are emitted.

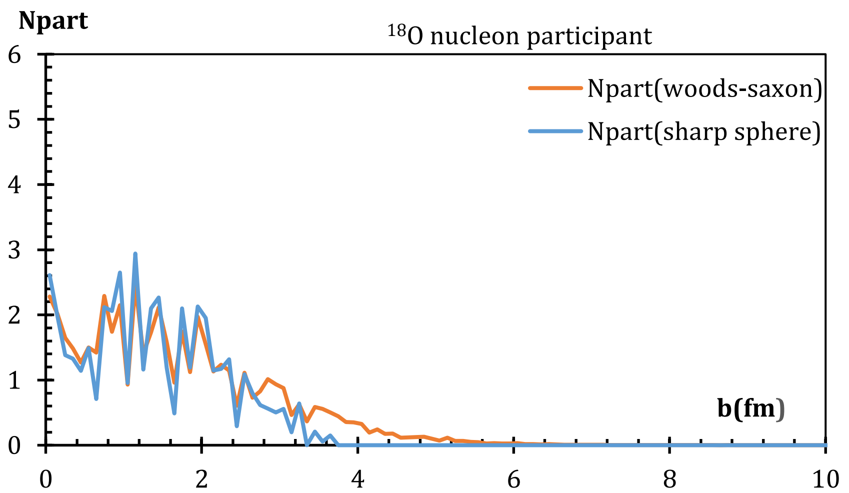

Figure 4. Number of nucleons that participate in the collision at *0.056TeV*

As illustrated in **Fig. 4**, the total number of participant nucleons in the Npart depends sensitively on which nuclear density distribution is used. The variation of N_{part} with impact parameter is observed in other approaches as well. The Woods-Saxon density profile predicts a more gradual dependence, so that some higher values are expected for more peripheral collision geometries. Conversely, a sharp-sphere density distribution causes the number of participant nucleons to exhibit a steeper decline with increasing b. In both density profiles, $N_{part} \rightarrow 0$ as b increases because the overlap of colliding nuclei decreases as the impact parameter increases. As a next step in the scattering process, the elastic DCS is calculated and shown in **Fig. 5**. The computed DCS describes elastic scattering events, for which the colliding particles remain in their ground states, i.e., with no internal excitation.

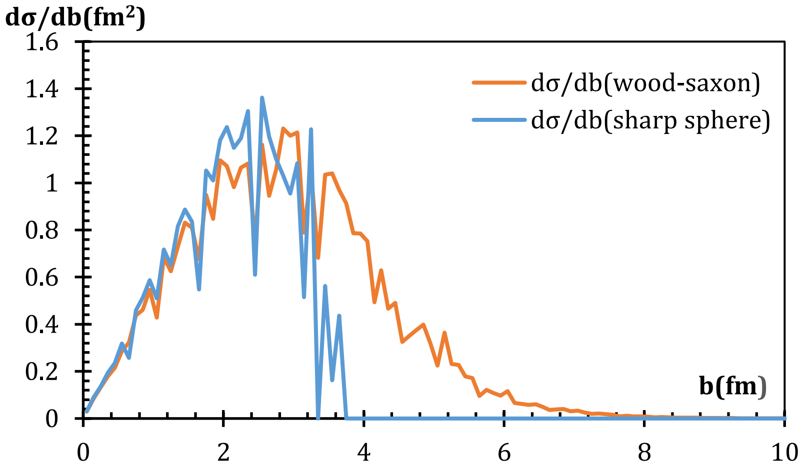

Figure 5. Differential cross section (DCS) concerning the impact parameter

The differential cross-section for particle collisions with a nucleus is influenced by various parameters, including the energy of the colliding particle, the features of the particles, the specific nucleus concerned, and the scattering angle. Resonant behavior is frequently seen in the cross-section energy dependence, with peaks and troughs aligned with certain energy levels in the oxygen nucleus. These resonances provide valuable insights into the nuclear structure and excitation spectra of the oxygen nucleus. The normalized integral cross section for collisions within the two types of distribution is illustrated in **Fig. 6**. It denotes the probability of a collision happening for a specified impact parameter. When the impact parameter is large, that indicates the collision is more peripheral.

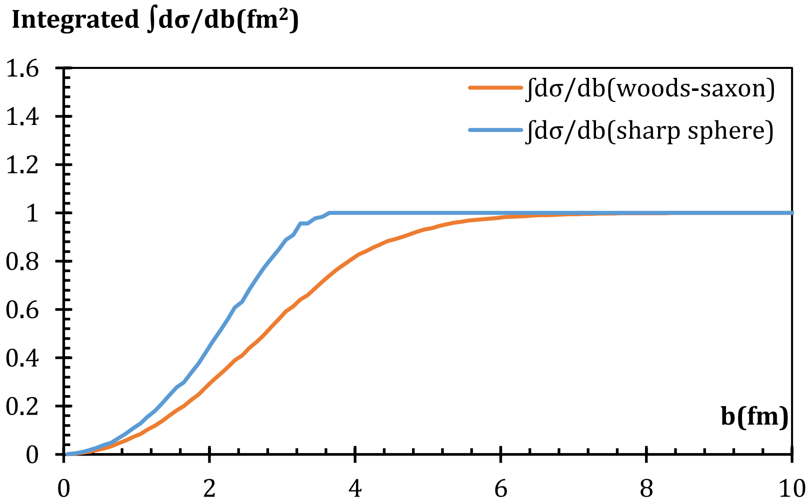

Figure 6. Normalized integral cross section for collisions in different energy ranges

The normalization of the cross-section signifies that the overall area below the curve equals one. The data points illustrated in this fig. represent the integral cross-section over various distributions; for example, the data point at approximately 2 *fm* with a collision energy of 0.3 *TeV* implies that the normalized integral cross-section is roughly 0.3. The curve's shape depends on the specific type of nuclear density distribution, whereas the Woods-Saxon curve exhibits a more gradual profile and attains saturation at about b ≈ 6 *fm*, while the Sharp-Sphere increases rapidly and attains saturation at roughly b ≈ 4 *fm*.

The proton and neutron have non-uniform internal mass distributions owing to their quark and gluon composition. At elevated energies, such as those attained at the Large Hadron Collider (CERN) and the Relativistic Heavy Ion Collider (RHIC), the internal structure of these nucleons becomes critically pertinent and profoundly affects the collision dynamics. This is most apparent in the proton, which can no longer be regarded as a mere spherical particle with a uniform matter distribution. Rather, it comprises discrete areas of elevated gluon density that vary from event to event, that is, from one collision to the next **(Mäntysaari, 2020).** These variations alter the effective shape and density profile of the colliding system, as evidenced in density distributions. Thus, the overlap region in p+O collisions dictates the resultant geometric configuration: a nearly circular overlap yields a modest eccentricity, whereas an elongated overlap results in a big eccentricity **(Alver et al., 2008).** The irregularity of this overlap zone stems from quark-level fluctuations, as quarks are subnuclear components that generate particle density distributions, collective flow, and notable event-by-event anisotropies in the produced particles. Experimental observations at the Large Hadron Collider and the Relativistic Heavy Ion Collider have validated these phenomena. Consequently, at elevated energy, the intrinsic quark–gluon composition of nucleons and their variations result in alterations to the geometric configuration of the collision. This effect is especially prominent in p+O collisions, as the system size is analogous to the typical scale of these oscillations, in contrast to larger collision systems **(Busza et al., 2018)**.

4. CONCLUSIONS

This study shows that the geometric properties of high-energy P-Oxygen ($\sqrt{s_{NN}}$=0.056 TeV) collisions are highly sensitive to the choice of nuclear density distribution. When analyzed within the Optical Glauber Model. The analysis was based on several key observables, including the thickness and overlap functions, the number of participant nucleons (Npart), and the number of binary collisions. A systematic comparison was performed between the Woods-Saxon distribution and the Sharp-Sphere distribution. The resulting data strongly indicate that the selected nuclear density profile essentially defines geometric properties for high-energy collisions. In particular, the Woods-Saxon distribution produces a more extended and smoother nuclear overlap area, resulting in a larger number of participant nucleons persisting over the entire range of impact parameters examined. In contrast, the Sharp-Sphere distribution results in a more abrupt decline in all values as the impact parameter increases, producing its sharply bounded nuclear density profile. Notwithstanding the change in the function used to generate these distributions, both distributions exhibit a monotonic decrease with increasing impact parameter that is directly correlated with overlaps of colliding nuclei. In addition, this study highlights the particular significance of the Oxygen nucleus as a light-mass system. The oxygen nucleus serves as an important light-mass reference system for studying proton-nucleus interactions. This is an area that has not been heavily scrutinized in comparative studies of nuclear density distributions. These results demonstrate that the geometric properties of the initial state are sensitive to the assumed shape of nuclear matter. The Glauber Model requires the use of accurate and realistic nuclear structure models to properly describe the initial state of high-energy collisions. This shows clearly how crucial it is to use accurate and realistic models of nuclear structure when building theoretical frameworks for collisions within the Glauber Model.

Credit Authorship Contribution Statement

Israa Ali Madi: Conceptualization, Methodology, Investigation, Formal analysis, Software, Data curation, Visualization, Writing – original draft. Basim Khalaf Rejah: Writing – review & editing, Validation.

Declaration of Competing Interests

The authors declare that they have no known competing financial interests or personal relationships that could have appeared to influence the work reported in this paper.

REFERENCES

Aaij, R., Abellán Beteta, C., Ackernley, T., Adeva, B., Adinolfi, M., Afsharnia, H., Aidala, C.A., Aiola, S., Ajaltouni, Z., Akar, S. and Albrecht, J., 2022. Centrality determination in heavy-ion collisions with the LHCb detector. *Journal of Instrumentation*, *17*(05), P. P05009. https://doi.org/10.1088/1748-0221/17/05/P05009

Ali, A.M. and Mohammed, H.M., 2022. Determination of differential cross-section of (n+89Y) elastic and inelastic scattering using Eikonal approximation. *Iraqi Journal of Science*, pp. 2514–2522. https://doi.org/10.24996/ijs.2022.63.6.18.

Ali, H. and Ali, A., 2025. Proton-Pb collision utilizing Woods-Saxon density shape within optical Glauber model. *Journal of University of Anbar for Pure Science*, 19(1), pp. 219–225. https://doi.org/10.37652/juaps.2024.152975.1312.

Ali, H.A. and Ali, A.M., 2025. D-Au collision at different $\sqrt{s_{NN}}$ (GeV) using Woods-Saxon density shape within the optical Glauber model. In: *6th International Conference for Physics and Advance Computation Sciences: ICPAS2024*. Baghdad, Iraq, P. 050034. https://doi.org/10.1063/5.0267500

Alver, B., Back, B.B., Baker, M.D., Ballintijn, M., Barton, D.S., Betts, R.R., Bindel, R., Busza, W., Chetluru, V., García, E. and Gburek, T., 2008. The importance of correlations and fluctuations on the initial source eccentricity in high-energy nucleus-nucleus collisions. *Physical Review C*, 77(1), P. 014906. https://doi.org/10.1103/PhysRevC.77.014906.

Alvioli, M., Cole, B., Frankfurt, L., Perepelitsa, D. and Strikman, M., 2014. Evidence for x-dependent proton color fluctuations in pA collisions at the LHC. *arXiv preprint* arXiv:1409.7381. [online]. https://doi.org/10.48550/ARXIV.1409.7381.

Alvioli, M., Frankfurt, L., Perepelitsa, D. and Strikman, M., 2017. Global analysis of color fluctuation effects in proton- and deuteron-nucleus collisions at RHIC and the LHC. *arXiv preprint*, arXiv:1709.04993 [online]. https://doi.org/10.48550/ARXIV.1709.04993.

Andronic, A. and Arnaldi, R., 2025. Quarkonia and deconfined Quark–Gluon Matter in heavy-Ion collisions. *Annual Review of Nuclear and Particle Science*, 75(1), pp. 351–375. https://doi.org/10.1146/annurev-nucl-121423-101041.

Busza, W., Rajagopal, K. and Schee, W. van der, 2018. Heavy Ion collisions: The big picture, and the big questions. *Annual Review of Nuclear and Particle Science*, 68(1), pp. 339–376. https://doi.org/10.1146/annurev-nucl-101917-020852.

Brueckner, K.A., Buchler, J.R., Jorna, S. and Lombard, R.J., 1968. Statistical theory of Nuclei. *Physical Review*, 171(4), pp. 1188–1195. https://doi.org/10.1103/PhysRev.171.1188.

CMS Collaboration, 2025. Discovery of suppressed charged-particle production in ultrarelativistic oxygen-oxygen collisions. *arXiv preprint*, arXiv:2510.09864. https://doi.org/10.48550/ARXIV.2510.09864.

d'Enterria, D. and Loizides, C., 2021. Progress in the Glauber Model at collider energies. *Annual Review of Nuclear and Particle Science*, 71(1), pp. 315–344. https://doi.org/10.1146/annurev-nucl-102419-060007.

Eskola, K.J., Paakkinen, P., Paukkunen, H. and Salgado, C.A., 2017. EPPS16: Nuclear parton distributions with LHC data. *The European Physical Journal C*, 77(3), P. 163. https://doi.org/10.1140/epjc/s10052-017-4725-9.

Iancu, E., 2012. QCD in Heavy Ion Collisions. *arXiv preprint*, arXiv:1205.0579. https://doi.org/10.48550/ARXIV.1205.0579.

LHCb collaboration, 2022. Centrality determination in heavy-ion collisions with the LHCb detector. *Journal of Instrumentation*, 17(5), P. P05009. https://doi.org/10.1088/1748-0221/17/05/P05009

Jia, J., 2009. Influence of the nucleon-nucleon collision geometry on the determination of the nuclear modification factor for nucleon-nucleus and nucleus-nucleus collisions. *Physics Letters B*, 681(4), pp. 320–325. https://doi.org/10.1016/j.physletb.2009.10.044.

Kasza, G.L., 2026. Thermal radiation from an analytic hydrodynamic model with Hadronic and Quark-Gluon Plasma sources in Heavy-Ion collisions. *Progress of Theoretical and Experimental Physics*, 2026 (3), P. 033D01. https://doi.org/10.48550/arXiv.2507.13240

Krupczak, R., Borghini, N. and Roch, H., 2025. Mode-by-mode evolution of Pb-Pb collisions at 5.02 TeV in a hybrid model. *arXiv preprint*, arXiv:2508.05336. https://doi.org/10.48550/ARXIV.2508.05336.

Kumar, V. and Shukla, P., 2024. Quantifying the jet energy loss in Pb+Pb collisions at LHC. *The European Physical Journal A*, 60(8), P. 169. https://doi.org/10.1140/epja/s10050-024-01393-5.

Kuttan, M.O., Steinheimer, J., Zhou, K., Bleicher, M. and Stoecker, H., 2023. Model dependence of the number of participant nucleons and observable consequences in Heavy-Ion collisions. *arXiv preprint,* arXiv:2303.07919[online]. https://doi.org/10.48550/ARXIV.2303.07919.

Liu, L.-M., Zhang, C.-J., Xu, J., Jia, J. and Peng, G.-X., 2022. Free spectator nucleons in ultracentral relativistic heavy-ion collisions as a probe of neutron skin. *Physical Review C*, 106(3), P. 034913. https://doi.org/10.1103/PhysRevC.106.034913.

Loizides, C., Nagle, J. and Steinberg, P., 2015. Improved version of the PHOBOS Glauber Monte Carlo. *SoftwareX*, 1–2, pp. 13–18. https://doi.org/10.1016/j.softx.2015.05.001.

Loizides, C., Kamin, J. and d'Enterria, D., 2018. Improved Monte Carlo Glauber predictions at present and future nuclear colliders. *Physical Review C*, 97(5), P. 054910. https://doi.org/10.1103/PhysRevC.97.054910.

Mäntysaari, H., 2020. Review of proton and nuclear shape fluctuations at high energy. *Reports on Progress in Physics*, 83(8), P. 082201. https://doi.org/10.1088/1361-6633/aba347.

Mattioli, K.R., 2024. Towards experimental confirmation of Quarkonia melting in Quark–Gluon Plasma: A review of recent measurements of Quarkonia production in relativistic Heavy-Ion Collisions. *Symmetry*, 16(2), P. 225. https://doi.org/10.3390/sym16020225.

Mehndiratta, A. and Shukla, P., 2017. The Glauber model and heavy ion reaction and elastic scattering cross sections. *Nuclear Physics A*, 961, pp. 22–36. https://doi.org/10.1016/j.nuclphysa.2017.02.002.

Mifsud, J., 2013. Optical Glauber modeling in high-energy nuclear collisions. *XJENZA On line*, (2), pp. 66–72. https://doi.org/10.7423/XJENZA.2013.2.08.

Miller, M.L., Reygers, K., Sanders, S.J. and Steinberg, P., 2007. Glauber Modelling in high-energy nuclear collisions. *Annual Review of Nuclear and Particle Science*, 57(1), pp. 205–243. https://doi.org/10.1146/annurev.nucl.57.090506.123020.

Nasim, Md., Shi, S., Chatterjee, S., Singha, S. and Roy, V., 2017. Collectivity in high energy Heavy-Ion Collisions. *Advances in High Energy Physics*, 2017, pp. 1–2. https://doi.org/10.1155/2017/1485353.

Nguyen, M., 2020. Heavy-Ion physics. *CERN Yellow Reports: School Proceedings*, 5, P. 129. https://doi.org/10.23730/CYRSP-2020-005.129.

Perepelitsa, D.V., 2024. Contribution to differential π^0 and γ_{dir} modification in small systems from color fluctuation effects. *arXiv preprint*, arXiv:2404.17660. https://doi.org/10.48550/ARXIV.2404.17660.

Ramasubramanian, N., 2021. Validation of the Glauber model for centrality determination in small system collisions. *Zenodo,* P. 5919235. https://doi.org/10.5281/ZENODO.5919235.

Salgado, C.A., Alvarez-Muniz, J., Arleo, F., Armesto, N., Botje, M., Cacciari, M., Campbell, J., Carli, C., Cole, B., D'Enterria, D. and Gelis, F., 2011. Proton-Nucleus Collisions at the LHC: Scientific opportunities and requirements. *arXiv preprint*, arXiv:1105.3919. https://doi.org/10.48550/ARXIV.1105.3919.

Segal, I., 2023. Centrality determination in Heavy-Ion collisions based on Monte-Carlo sampling of spectator fragments. *Particles*, 6(2), pp. 568–579. https://doi.org/10.3390/particles6020032.

Shukla, P., 2001. Glauber model for heavy ion collisions from low energies to high energies. *arXiv preprint*, arXiv:nucl-th/0112039. https://doi.org/10.48550/arXiv.nucl-th/0112039.

Wong, C.-Y., 1994. *Introduction to High-Energy Heavy-Ion Collisions*. World Scientific Publishing Co. Pte. Ltd. eBooks. https://doi.org/10.1142/9789814277549.

دراسة تصادم البروتون والأوكسجين بناءً على توزيع كثافة وودز–ساكسون وشارب–سفير ضمن إطار نموذج غلاوبر البصري

اسراء علي ماضي*، باسم خلف رجه

قسم علوم فيزياء، كلية العلوم للبنات، جامعة بغداد، بغداد، العراق

الخلاصة

تحلل هذه الدراسة تصادمات البروتون–الأوكسجين عند الطاقات العالية، وتقيّم تأثير اختلاف توزيع الكثافة النووية على النتائج. ويمكن تحقيق ذلك باستخدام نموذج وودز–ساكسون، الذي يتميز بتوزيع كثافة متناقص تدريجيًا من المركز إلى الحافة، ونموذج الكرة الحادة، الذي يعتمد على انخفاض حاد في توزيع الكثافة من مركز النواة إلى محيطها. وتناقش النتائج تصادمات البروتون–الأوكسجين عند طاقة مركز الكتلة $\sqrt{s_{NN}}$ =0.056 تيرا إلكترون فولت، باستخدام طريقة غلاوبر البصرية. يصف هذا النظام النواة كمادة متجانسة دون أي حدود واضحة أو تغيرات سريعة في الكثافة، مع الأخذ في الاعتبار أن عملية التفاعل بأكملها تُجرى تحليليًا. ويمكن فهم العديد من تصادمات البروتون–الأوكسجين عالية النسبية من خلال جهد المذبذب التوافقي، وفقًا لإطار عمل نموذجي وودز–ساكسون والكرة الحادة لنوى الأوكسجين. وبعد التصادم، تزداد دالة السماكة. تكون دالة التداخل ذات قيم عالية عند أدنى قيمة لمعامل التأثير، والعكس صحيح. فعندما يزداد معامل التأثير، تنخفض دالة التداخل. وبسبب تأثيرات تقلبات الانحراف، يتناقص عدد النيوكليونات التي يتم رصدها من قبل النواتج المشاركة (Npart) والنواتج الناتجة عن التصادم الثنائي (Ncoll) في منطقة التصادمات المحيطية مع ازدياد معامل التأثير (b).

الكلمات المفتاحية:تصادمات الأيونات الثقيلة، طاقة عالية، كثافة نووية، نصف قطر نووي، بلازما الكوارك–غلوون.